Gallery of Fluid Motion

High-speed and infrared imaging of frost propagation on breath figures

David Paulovics ,[1,*] Christophe Raufaste ,[1,2] Thomas Frisch ,[1]
Cyrille Claudet ,[1] and Franck Celestini [1]
[1] *Université Cote d'Azur, CNRS, Institut de Physique de Nice, Nice, France*
[2] *Institut Universitaire de France (IUF), Paris, France*

(Received 10 June 2024; published 22 November 2024)

This paper is associated with a video winner of a 2023 American Physical Society's Division of Fluid Dynamics (DFD) Milton van Dyke Award for work presented at the DFD Gallery of Fluid Motion. The original video is available online at the Gallery of Fluid Motion, https://doi.org/10.1103/APS.DFD.2023.GFM.V0079.

DOI: 10.1103/PhysRevFluids.9.110507

Frost formation on surfaces is a common phenomenon in cold and humid environments. The various mechanisms involved in this process are subjects of ongoing research due to their fundamental importance and practical implications for frost control in areas such as aircraft safety, heat pumps, power lines, and wind turbines [1–6]. Despite these efforts, understanding the dynamics of frost formation on a simple flat surface remains challenging due to the complexity of the multiphase and multiscale system involved. In humid conditions, water condenses on cold surfaces, forming assemblies of droplets called breath figures [7]. When the temperature is lowered below 0 °C, condensation frosting occurs, characterized by the freezing of the water droplets [3,8]. In this paper, we focus on the dynamics of frost propagation within breath figures. In particular, we present images highlighting recent results obtained from experiments combining high-speed microscopy and infrared imaging [9].

Breath figures were obtained through dropwise condensation on a partially wetting substrate. On such a substrate, droplets nucleate and grow by coalescence and by direct growth from humidity. The droplets in breath figures exhibit a bimodal size distribution. The first mode consists of small droplets that nucleate in the free spaces between larger ones, while the second mode comprises larger droplets that grow through coalescence with smaller droplets and with each other [7,10]. We characterize breath figures by the mean radius of the larger droplets in the second mode. In our experiments, breath figure samples were prepared on polycarbonate substrates cooled to 5 °C in a chamber where temperature and relative humidity were controlled to 25 °C and 80%, respectively. The chamber used was a vertical laminar flow hood, where humidity was regulated with a $\pm 2\%$ precision using a hygrostat controlling an ultrasonic water nebulizer. The size of condensed droplets was controlled by varying the duration that the sample remained in the condensation chamber, from 10 s to 5 h. Using this approach, we achieved mean droplet radii ranging from 10 to 1000 μm. Figure 1 displays an image sequence of a breath figure taken at successive time intervals of 20 min.

[*]Contact author: david.paulovics@univ-cotedazur.fr

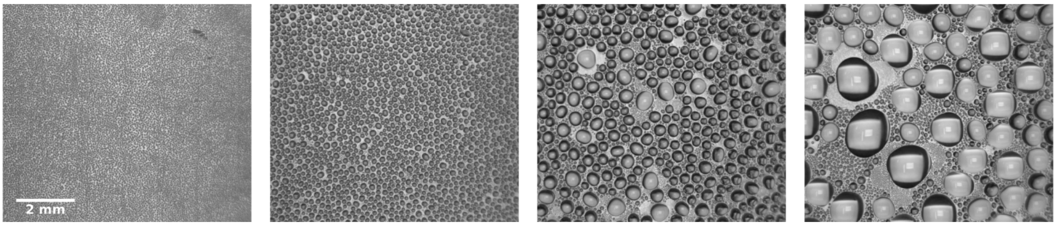

FIG. 1. Stages of breath figure formation on a horizontal surface. Each snapshot was taken at 20-min intervals.

Once the breath figure formed, we placed the sample on a Peltier stage and cooled it to $-20\,^{\circ}$C in 2 min. We then imaged it from above using a high-speed infrared camera (FLIR X6980). In Fig. 2, four successive infrared snapshots extracted from our video [11] illustrate the propagation of a circular pattern made of bright discs corresponding to freezing droplets. These "flashes" in the infrared images are associated with the release of latent heat during the freezing process and mark the frontier between an inner region of frozen droplets and an outer region where the droplets are still liquid.

Figure 3 shows the freezing process at the scale of a single droplet. The upper part of the figure shows side-view images of the droplet at different stages of the process, while the lower part presents the simultaneous top-view infrared images. The first image, taken 4 ms before solidification begins, shows the liquid droplet in its initial supercooled state at a temperature close to $-20\,^{\circ}$C. In the second and third images, we see a solidification front initiated at the contact with the substrate propagating vertically from bottom to top. In the corresponding infrared images, we observe that the temperature of the droplet increased to $0\,^{\circ}$C. The bright flashes in the infrared images can now be interpreted as the increase in temperature of the droplet during isothermal solidification. The temperature of the droplet stays approximately constant throughout the entire solidification process. The fourth image shows the solidified droplet, and we can see in the infrared image that the droplet has cooled and its temperature is again close to that of the surrounding substrate, $-20\,^{\circ}$C. The pointy form of the droplet tip after solidification is due to the lower density of solid water compared to liquid water [12].

In addition to the freezing process at the single droplet scale, we need to consider another mechanism to understand how frost can propagate from one droplet to another since they are not in direct contact. When a frozen droplet is in the vicinity of a liquid droplet, the difference in saturation vapor pressure between ice and supercooled water [13] causes the liquid droplet to evaporate and water vapor molecules to diffuse toward the frozen droplet. These molecules, supplied by the liquid droplet, deposit on the frozen droplet, forming ice dendrites growing toward the liquid droplet, forming ice bridges [3]. The growth process of these ice bridges is illustrated by an image sequence

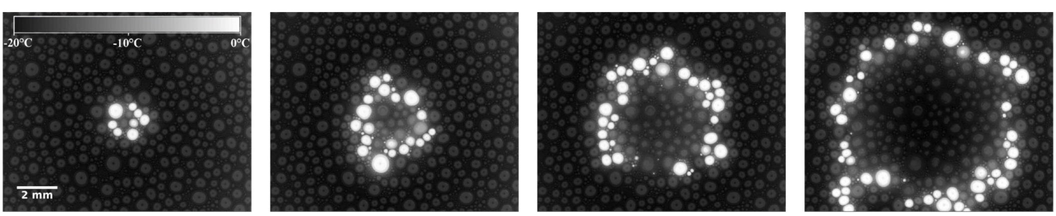

FIG. 2. Infrared images showing frost propagation inside a breath figure. Bright flashes indicate freezing droplets that exhibit a temperature increase, from $-20\,^{\circ}$C to $0\,^{\circ}$C, associated with the release of latent heat of solidification. These flashes separate an inner region of frozen droplets from an outer region of supercooled liquid droplets. Images were taken at 5-sec intervals from the onset of the first freezing event.

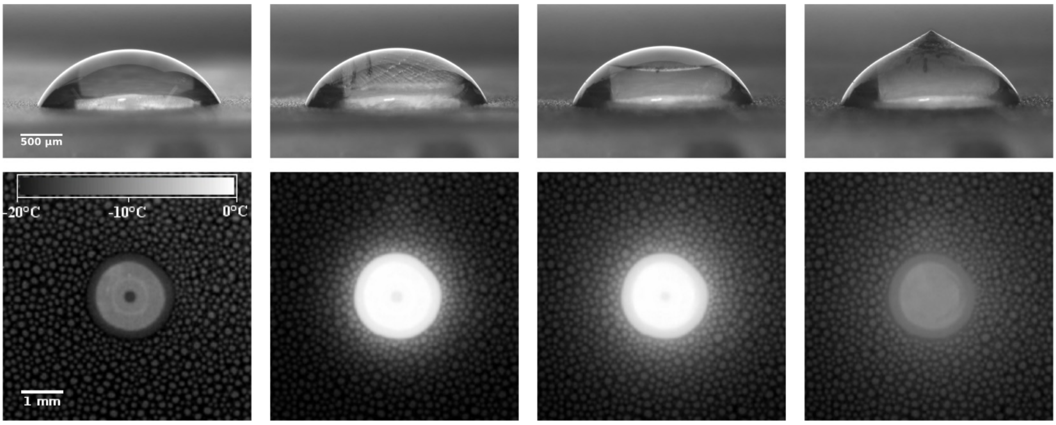

FIG. 3. Image sequence of a freezing droplet, combining simultaneous optical (side view) and infrared (top view) imagery. In the first image, we see a supercooled liquid droplet whose temperature is close to the substrate temperature, $-20\,^{\circ}$C. The second image is taken just after the initiation of the freezing process. A solidification front initiated at the contact with the substrate propagates upward. The displacement of the front is visible between the second and third images. This process occurs at $0\,^{\circ}$C, the temperature associated with the solidification isotherm, as shown by the bright flash in the infrared images. The fourth image is taken after solidification, where we see the pointy tip of the ice, and the infrared image shows that the droplet has cooled back to the surrounding temperature. Images were taken at 3-sec intervals.

in Fig. 4. The growth accelerates as the gap between the dendrite tip and the liquid droplet narrows [14]. Once an ice bridge makes contact with a liquid droplet, it serves as an ice nucleation site, causing the droplet to freeze as described previously. This chain reaction of freezing and ice bridge formation sets the dynamics of frost propagation. This process continues until frost covers the entire substrate.

In conclusion, the images presented in this paper reveal the mechanisms behind droplet cooling and freezing in condensation frosting. Characterizing these processes at the local scale of droplets is essential for understanding how these mechanisms compete to influence the dynamics of frost propagation on the global scale of the breath figure. Such images are crucial for understanding the effects of parameters such as temperature and the thermal conductivity of the substrate, as well as for refining models that describe droplet-droplet interactions. The experimental technique used here could also be applied to study condensation frosting under various conditions, with the aim of

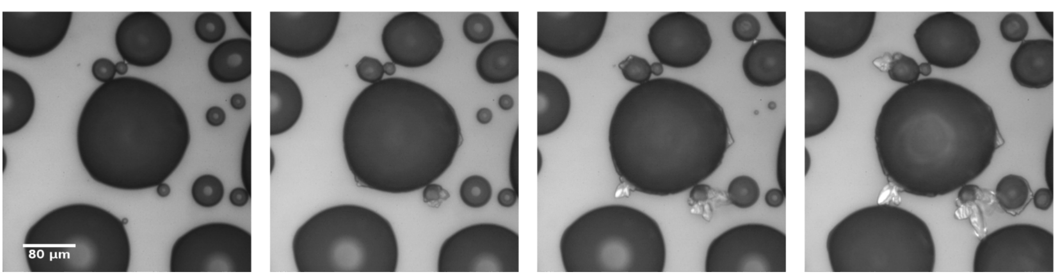

FIG. 4. An optical image sequence of ice bridge formation from a top view. Supercooled liquid droplets and frozen droplets can be distinguished by the presence or lack of optical reflection from their tops, respectively. Ice bridges grow from frozen droplets to liquid droplets. Once touched by an ice bridge, a supercooled liquid droplet starts freezing. One can notice interference fringes in the ice bridges, indicating a thickness of only a few micrometers. Images were taken at 0.5-sec intervals.

preventing or delaying frost formation. This includes utilizing ice-phobic [15] or superhydrophobic surfaces [16,17], which reduce the adhesion of ice and droplets to substrates.

We thank Médéric Argentina, Pierre Müller, and Stefano Curiotto for discussions and acknowledge support from the Doeblin Federation CNRS FR 2800.

---

[1] J. Petit and E. Bonaccurso, General frost growth mechanism on solid substrates with different stiffness, Langmuir **30**, 1160 (2014).

[2] S. Nath, S. F. Ahmadi, and J. B. Boreyko, A review of condensation frosting, Nanoscale and Microscale Thermophysical Engineering **21**, 81 (2017).

[3] S. Nath, S. F. Ahmadi, and J. B. Boreyko, How ice bridges the gap, Soft Matter **16**, 1156 (2020).

[4] Y. Zhao, Q. Guo, T. Lin, and P. Cheng, A review of recent literature on icing phenomena: Transport mechanisms, their modulations and controls, Int. J. Heat Mass Transfer **159**, 120074 (2020).

[5] A. Azimi Yancheshme, G. Momen, and R. Jafari Aminabadi, Mechanisms of ice formation and propagation on superhydrophobic surfaces: A review, Adv. Colloid Interface Sci. **279**, 102155 (2020).

[6] L. Hauer, W. S. Y. Wong, V. Donadei, K. I. Hegner, L. Kondic, and D. Vollmer, How frost forms and grows on lubricated micro- and nanostructured surfaces, ACS Nano **15**, 4658 (2021).

[7] D. Beysens and C. M. Knobler, Growth of breath figures, Phys. Rev. Lett. **57**, 1433 (1986).

[8] S. Chavan, D. Park, N. Singla, P. Sokalski, K. Boyina, and N. Miljkovic, Effect of latent heat released by freezing droplets during frost wave propagation, Langmuir **34**, 6636 (2018).

[9] D. Paulovics, C. Raufaste, T. Frisch, C. Claudet, and F. Celestini, Dynamics of frost propagation on breath figures, Langmuir **38**, 2972 (2022).

[10] D. Paulovics, E. Bormashenko, C. Raufaste, and F. Celestini, Quantifying order in breath figure patterns through Voronoi entropy, Phys. Rev. E **110**, 024302 (2024).

[11] The original video is available online at the gallery of fluid motion, https://doi.org/10.1103/APS.DFD.2023.GFM.V0079.

[12] X. Zhang, X. Wu, J. Min, and X. Liu, Modelling of sessile water droplet shape evolution during freezing with consideration of supercooling effect, Appl. Therm. Eng. **125**, 644 (2017).

[13] S. Nath and J. B. Boreyko, On localized vapor pressure gradients governing condensation and frost phenomena, Langmuir **32**, 8350 (2016).

[14] S. Curiotto, D. Paulovics, C. Raufaste, F. Celestini, T. Frisch, F. Leroy, F. Cheynis, and P. Müller, Atomistic description of interdroplet ice-bridge formation during condensation frosting, Langmuir **39**, 579 (2023).

[15] K. Golovin, S. P. Kobaku, D. H. Lee, E. T. DiLoreto, J. M. Mabry, and A. Tuteja, Designing durable icephobic surfaces, Sci. Adv. **2**, e1501496 (2016).

[16] J. B. Boreyko and C.-H. Chen, Self-propelled dropwise condensate on superhydrophobic surfaces, Phys. Rev. Lett. **103**, 184501 (2009).

[17] S. Jung, M. Dorrestijn, D. Raps, A. Das, C. M. Megaridis, and D. Poulikakos, Are superhydrophobic surfaces best for icephobicity? Langmuir **27**, 3059 (2011).